Comparison of simple potential functions for simulating liquid water

William L. Jorgensen, Jayaraman Chandrasekhar, Jeffry D. Madura, Roger W. Impey, and Michael L. Klein

Citation: J. Chem. Phys. **79**, 926 (1983); doi: 10.1063/1.445869
View online: http://dx.doi.org/10.1063/1.445869
View Table of Contents: http://jcp.aip.org/resource/1/JCPSA6/v79/i2
Published by the AIP Publishing LLC.

Comparison of simple potential functions for simulating liquid water

William L. Jorgensen, Jayaraman Chandrasekhar, and Jeffry D. Madura

Department of Chemistry, Purdue University, West Lafayette, Indiana 47907

Roger W. Impey and Michael L. Klein

Chemistry Division, National Research Council of Canada, Ottawa, Canada K1A OR6
(Received 14 March 1983; accepted 5 April 1983)

Classical Monte Carlo simulations have been carried out for liquid water in the NPT ensemble at 25 °C and 1 atm using six of the simpler intermolecular potential functions for the water dimer: Bernal–Fowler (BF), SPC, ST2, TIPS2, TIP3P, and TIP4P. Comparisons are made with experimental thermodynamic and structural data including the recent neutron diffraction results of Thiessen and Narten. The computed densities and potential energies are in reasonable accord with experiment except for the original BF model, which yields an 18% overestimate of the density and poor structural results. The TIPS2 and TIP4P potentials yield oxygen–oxygen partial structure functions in good agreement with the neutron diffraction results. The accord with the experimental OH and HH partial structure functions is poorer; however, the computed results for these functions are similar for all the potential functions. Consequently, the discrepancy may be due to the correction terms needed in processing the neutron data or to an effect uniformly neglected in the computations. Comparisons are also made for self-diffusion coefficients obtained from molecular dynamics simulations. Overall, the SPC, ST2, TIPS2, and TIP4P models give reasonable structural and thermodynamic descriptions of liquid water and they should be useful in simulations of aqueous solutions. The simplicity of the SPC, TIPS2, and TIP4P functions is also attractive from a computational standpoint.

I. INTRODUCTION

In view of the importance of water and aqueous solutions they will continue to be a principal subject for molecular dynamics and statistical mechanics simulations. The success of these investigations depends critically on the availability of intermolecular potential functions for the water dimer that yield a reasonable model for liquid water. A variety of functions has been proposed and tested to different extents.[1,2] Some of our recent efforts have been directed towards optimizing simple potential functions that may be rapidly evaluated in fluid simulations.[3,4] The results have been encouraging since simple functions have been developed that are generally as successful as any currently available ones for describing liquid water. In the present paper findings for six of the simpler functions are compared including the ST2,[5] Bernal–Fowler (BF),[6] and SPC[7] potentials and three developed at Purdue, TIPS2, TIP3P, and TIP4P. For each function, Monte Carlo simulations have been carried out for liquid water in the NPT ensemble at 25 °C and 1 atm. Self-diffusion coefficients have also been obtained from molecular dynamics simulations with several of the potential functions. Except for the BF model, the computed thermodynamic properties including densities are in reasonable accord with experimental data. In addition, the structural analyses include the first comparisons between theoretical results for all three partial structure functions and the recent neutron diffraction data of Thiessen and Narten.[8] The agreement between experiment and the TIPS2 and TIP4P models for the oxygen–oxygen (OO) partial structure function is particularly good. The lesser accord for the OH and HH partial structure functions and differences in the radial functions illuminate some of the uncertainties in comparing the calculation and experimental structural results. Hydrogen bonding analyses are also reported and emphasize the basic similarity of the calculated descriptions of liquid water.

II. POTENTIAL FUNCTIONS

The potential functions considered here all involve a rigid water monomer that is represented by three, four, or five interaction sites. The original TIPS 3 site model[3] has positive charges on the hydrogens and a negative charge on oxygen ($q_O = -2q_H$). The Coulombic interactions between all intermolecular pairs of charges along with a single Lennard-Jones term between oxygens determine the dimerization energy for monomers m and n, ϵ_{mn}, as given by Eq. (1). The parameters

$$\epsilon_{mn} = \sum_{i}^{\text{on } m} \sum_{j}^{\text{on } n} \frac{q_i q_j e^2}{r_{ij}} + \frac{A}{r_{OO}^{12}} - \frac{C}{r_{OO}^{6}} \tag{1}$$

(q_H, A, and C) were chosen to yield reasonable structural and energetic results for gas phase complexes of water and alcohols and for liquid water.[3]

Subsequently, Berendsen and co-workers used the same model, but optimized the parameters more thoroughly for liquid water.[7] The resultant "SPC" potential yields a better energy for liquid water than the TIPS and a small second peak in the OO radial distribution function (g_{OO}), though the first peak is in poorer accord with x-ray data than from the TIPS. More recently we also reparametrized the 3-point model to improve the energy and density for liquid water. This parametrization will be referred to as the TIP3P potential. However, as discussed in the Results section, the occurrence of the second peak in g_{OO} is sensitive to the computed density and tends to vanish for the 3-site model as this property is improved.

 0021-9606/83/140926-10$02.10

TABLE I. Monomer geometry and parameters for potential functions.

	SPC	TIP3P	BF	TIPS2	TIP4P
r(OH), Å	1.0	0.9572	0.96	0.9572	0.9572
∠HOH, deg	109.47	104.52	105.7	104.52	104.52
$A\times10^{-3}$, kcal Å^{12}/mol	629.4	582.0	560.4	695.0	600.0
C, kcal Å^6/mol	625.5	595.0	837.0	600.0	610.0
q(O)	−0.82	−0.834	0.0	0.0	0.0
q(H)	0.41	0.417	0.49	0.535	0.52
q(M)	0.0	0.0	−0.98	−1.07	−1.04
r(OM), Å	0.0	0.0	0.15	0.15	0.15

Consequently, 4-site models were investigated and found to be superior. In this case the negative charge is moved off the oxygen and towards the hydrogens at a point (M) on the bisector of the HOH angle. Equation (1) still applies with little increase in complexity: Ten distances are now required to evaluate the function instead of nine for the 3-site model. This 4-site form was first proposed by Bernal and Fowler along with a set of parameters based on calculations for properties of the monomer, dimer, and ice.[6] A different monomer geometry and parameters are used in the TIPS2 potential which was optimized for liquid water.[4] An alternative parametrization TIP4P has also been investigated that yields a slightly higher density than TIPS2, as discussed below. The monomer geometries and parameters for the five potential functions (SPC, TIP3P, BF, TIPS2 and TIP4P) are summarized in Table I.

The remaining function considered here is the extensively studied ST2 potential of Stillinger and Rahman.[5] It uses a 5-site model with charges on the hydrogens and on two lone pair positions oriented tetrahedrally around the oxygen. Again a single Lennard-Jones term is included and acts between the oxygens. The extra site increases the complexity so that 17 distances are required to evaluate the potential function. As a consequence, the total computer time for a Monte Carlo simulation with the ST2 potential is about 35% more than with one of the 3- or 4-site alternatives. This is a significant factor since a typical simulation of one pressure and temperature may require 3–7 days on a VAX-like computer.

Each potential function yields a linear water dimer as the lowest energy hydrogen bonded form. The optimal geometric parameters and dimerization energies are listed in Table II. As usual, θ is the angle between the HOH bisector of the hydrogen bond acceptor and the hydrogen bond vector. The maximal hydrogen bond strengths are all 6–7 kcal/mol with the ST2 value highest at 6.84 kcal/mol. The ST2 model also yields the longest OO separation (2.85 Å), while the BF function has the shortest (2.72 Å). The 3-site models yield a flatter dimer ($\theta=26°$–$27°$) than the 4- and 5-site functions (46°–52°). The latter values are closer to the microwave result for the gas phase dimer (60°)[9]; however, the experimental OO distance (2.98 Å)[9] and dimerization energy (5.44 ± 0.7 kcal/mol)[10] do not agree closely with the results from the potential functions. The discrepancies are necessary for the potential functions to provide reasonable thermodynamic and structural results for liquid water in the absence of explicit three-body corrections. Thus, the functions are all effective pair potentials.

III. COMPUTER SIMULATIONS

The statistical mechanics calculations were carried out with the six potential functions in the NPT ensemble at 25 °C and 1 atm. The computational formalism has been described previously.[11] The essential details are that the Monte Carlo simulations were executed using cubic samples of 125 monomers, periodic boundary conditions, and Metropolis sampling. Spherical cutoffs at 7.5 Å were used in evaluating the dimerization energies which includes interactions with a monomer's ~60 nearest neighbors. New configurations were generated by randomly translating and rotating a randomly chosen monomer. In addition, the volume of the system was changed randomly on every 600th attempted move and all coordinates were scaled appropriately. The sampling is then based on Eq. (2) where the subscripts n and o refer to the new and old

$$\Delta W=(E_n-E_o)+P(V_n-V_o)-NkT\ln(V_n/V_o) \qquad (2)$$

configuration.[11] If $\Delta W\leq0$ or it $\exp(-\Delta W/kT)>X$ where X is a random number between 0 and 1, then the new configuration is accepted, otherwise it is rejected.[11] The ranges for the translations (±0.15 Å), rotations (±15°) and volume changes (±50 Å^3) were chosen to provide acceptance rates of ~40% for new configurations. The simulations were initiated using liquid configurations from earlier runs. In each case, equilibration involved at least 500 K configurations and averaging was carried out over an additional 1000 K configurations.

TABLE II. Optimized geometry and dimerization energy for the linear water dimer.

Potential	r(OO), Å	θ, deg	$-\Delta E$, kcal/mol
SPC	2.75	26	6.59
TIP3P	2.74	27	6.50
BF	2.72	47	6.06
ST2	2.85	52	6.84
TIPS2	2.79	46	6.20
TIP4P	2.75	46	6.24

TABLE III. Calculated and experimental properties for liquid water at 25°C and 1 atm.[a]

	SPC	TIP3P	BF	TIPS2	TIP4P	ST2	Expt.[b]
d(g/cm^3)	0.971	0.982	1.181	0.927	0.999	0.925	0.997
$-E_t$ (kcal/mol)	10.18	9.86	10.49	9.88	10.07	10.37	9.92[c]
ΔH_{vap} (kcal/mol)	10.77	10.45	11.08	10.47	10.66	10.96	10.51
C_p (cal/mol deg)	23.4	16.8	16.0	18.9	19.3	22.2	17.99
$10^5\,\alpha$ (deg^{-1})	58	41	59	88	94	−69	25.7
$10^6\,\kappa$ (atm^{-1})	27	18	18	56	35	63	45.8

[a]No cutoff corrections have been made to the computed properties.
[b]See Refs. 4 and 12.
[c]See the text.

Molecular dynamics calculations were also undertaken in order to investigate the adequacy of the dynamic properties for the Bernal–Fowler type models. These simulations were carried out using 125 water molecules in a cube with the density fixed at 1.0 g cm^{-3} and with periodic boundary conditions. Corrections were made for the long-range electrostatic interactions by an Ewald method, while the short-range interactions were truncated at 7.75 Å. Self-diffusion coefficients were obtained by monitoring the displacement of a molecule as a function of time, averaging over all molecules and all choices of time origins, and using the Einstein relation, $6D = \lim_{t\to\infty}(d/dt) \times \langle |r_i(t) - r_i(0)|^2 \rangle$. The results are based on averages over 6000 time steps covering 10 ps.

IV. RESULTS AND DISCUSSION

A. Thermodynamics

The thermodynamic results from the simulations are compared with experimental data in Table III. The experimental results are taken from compilations[12] except for the intermolecular energy E_t whose origin is discussed below. The estimation of the statistical uncertainties for the computed properties has been analyzed previously.[13] In the present case, the error bars ($\pm 1\sigma$) are approximately ± 0.007 g cm^{-3} for d, ± 0.03 kcal/mol for E_t and ΔH_{vap}, ± 2 cal/mol deg for C_p, and $\pm 8\times10^{-6}$ atm^{-1} for κ. The fluctuation properties, C_p and κ converge relatively slowly and the values in Table III may be 10%–20% below the true figures.[13] Furthermore, α converges so slowly that little significance can be attached to the computed results.

It should be noted that the computed values do not include any cutoff corrections. They are reported this way since there is no generally accepted means for making the cutoff corrections, though several procedures have been used previously.[5,14–16] In any event, the cutoff corrections and size dependence for the results discussed here should not be large based on previous studies.[5,13–18] For example, with systems of the present size cutoff corrections typically lower the total energy by 2%–3%.[4,5,14] For NVT simulations, the correction for the pressure has received little attention; it is probably less than 1000 atm which corresponds to an increase of 0%–4% in the density for water at 25 °C.[5,15] The small size dependence of the results for systems with 125 or 216 monomers has been noted previously.[13,17,18] It was confirmed again here by a Monte Carlo calculation for the TIP4P potential with 216 monomers that covered 3000 K configurations. Although the cutoff was increased from 7.5 to 8.5 Å in going from $N = 125$ to 216, the computed energy and density only change from -10.07 to -10.02 kcal/mol and 0.999 to 0.983 g cm^{-3}. The pattern is the same as found for the TIPS2 potential.[13] Interestingly it is opposite to what is generally expected for the cutoff corrections as described above. Of course, the expected trend may reemerge as the cutoff distance is increased further, though it is possible that the long range dipole–dipole correction is net repulsive for some potential functions.[14] The size dependence of the results for the fluctuation properties with the TIP4P potential was also small. With $N = 216$, the computed C_p, α, and κ are 18.5 cal/mol deg, 84×10^{-5} deg^{-1} and 42×10^{-6} atm^{-1}. The agreement with the values for C_p and κ in Table III is within the statistical limits of the calculations, while the accord for α is fortuitous.[13]

In comparison to experiment the errors in the uncorrected densities for the potential functions are SPC (3%), TIP3P (2%), BF (18%), TIPS2 (7%), TIP4P (0%), and ST2 (7%). The underestimate of the density with the ST2 potential is consistent with NVT simulations in which the truncated potential was found to yield a pressure of +534 atm at 10 °C.[15] Overall, the computed densities with or without cutoff corrections are in reasonable accord with experiment except for the BF potential. The high density for this function results from its shorter hydrogen bond (Table II) and its large Lennard-Jones C parameter (Table I) which broadens the hydrogen bond potential well. It should also be noted that the previously reported densities from the TIPS2 potential are 7% higher than the value in Table III.[4,13] The discrepancy is due to the fact that the previous simulations were inadvertently run at 1350 atm rather than 1 atm. Aside from the density, this change has an insignificant effect on the other computed thermodynamic and structural results discussed previously.[4,13]

The computed intermolecular energy and heat of vapor-

ization may be related by $\Delta H_{vap} = -E_t + P[V(g) - V(l)]$ which leads to the commonly quoted "experimental" E_t of −9.92 kcal/mol at 25 °C and 1 atm.[14,16,19] However, this assumes that the sum of the kinetic and vibrational energies for the liquid and gas are the same and that the gas is ideal.[4,20] Though the latter assumption is justified,[4] the former is not well established. A pertinent analysis has recently been provided by Berens *et al.* in the course of computing quantum corrections for the thermodynamic properties of liquid water from molecular dynamics simulations.[20] Though they do not report the quantum corrected energy of the gas, their results are consistent with an experimental intermolecular energy of −10.0 to −10.5 kcal/mol for the liquid.[20] Consequently, the computed intermolecular energies from the six potential functions in Table III are all reasonable estimates. It may be noted that the value for the ST2 potential (−10.4 kcal/mol) is in accord with other determinations mostly at 10 °C which range from −10.4 to −10.6 kcal/mol, even though there is substantial variation in system sizes, cutoff distances, boundary conditions, ensembles, and computational procedure.[1,2,5,15,17,18]

The computed C_P's reported in Table III have been augmented by $3R$ (6 cal/mol deg) for the classical kinetic energy contributions from translation and rotation of the monomers. The quantum corrected contribution has been estimated as 3.6 cal/mol deg[14]; the difference of 2.4 cal/mol deg would probably be offset in a longer simulation based on previous experience.[13,17] The computed C_P's are in good agreement with experiment in view of these uncertainties and of the statistical fluctuations (±2 cal/mol deg) except for the SPC and ST2 values which are too high. These two functions also lead to significant overestimates of C_V in simulations at constant volume.[2,5,7,15,17,18]

The computed isothermal compressibilities are in the right range; however, the 3-site models yield underestimates. The TIPS2 and ST2 potentials both overestimate κ which may be related to their similar underestimates of the density. Remarkably, the κ computed here with the ST2 potential is in exact accord with the results of Stillinger's and Rahman's molecular dynamics calculations extrapolated to 25 °C.[5] The TIP4P potential yields the best estimate of the compressibility and it should improve a little in a longer run.[13]

In view of the slow convergence of the coefficient of thermal expansion, little comment on the computed values is warranted. The negative value for the ST2 potential may be real since Stillinger and Rahman estimated that the ST2 potential yields a temperature of maximum density (TMD) a little above 25 °C.[5] The TIPS2 potential was also found to yield a TMD at 25 ± 25 °C under similar conditions as the ST2 potential.[4] Locating the TMD is difficult since it is a relatively small effect and because of the statistical uncertainties in computing the density.[4]

Overall, the six potential functions yield reasonable thermodynamic results for liquid water at 25 °C and 1 atm with one clear-cut exception, the density from the BF potential.

B. Self-diffusion coefficients

The self-diffusion coefficients calculated here for the original BF potential at 21 °C and TIPS2 at 20 °C are 4.3 and 3.2, respectively, in units of 10^{-5} cm^2/s and with uncertainties of ~±10%. These values may be compared with the SPC result at 27 °C (3.6),[7] the ST2 finding at 10 °C (1.9),[5] and experimental data at 15 (1.78) and 25 °C (2.30).[12(c)] Thus, these models all yield significant overestimates of D with the least error occurring with the ST2 potential. It might be tempting to rationalize the smaller self-diffusion coefficient for the ST2 model by noting its deeper hydrogen bonding well (Table II) and the greater structure it yields for liquid water (*vide infra*). However, this analysis appears oversimplified because the revised central force model of Stillinger and Rahman, which is a 3-site potential, yields a less structured liquid than ST2 and a self-diffusion coefficient that is much too low (1.1 at 29.5 °C).[16]

C. Structure

An important description of structure in a liquid is provided by radial distribution functions $g_{\alpha\beta}(r)$ and partial structure functions $a_{\alpha\beta}(k)$ which may be determined by diffraction experiments. The two functions are related by Eq. (3) where $j_0(z) = (\sin z)/z$, ρ is the bulk density, and $k = (4\pi/\lambda)\sin\theta$:

$$a_{\alpha\beta}(k) = \rho h_{\alpha\beta}(k) = 4\pi\rho \int_0^\infty [g_{\alpha\beta}(r) - 1] r^2 j_0(kr)\, dr \qquad (3)$$

is the momentum transfer coordinate for elastic scattering of radiation with wavelength λ at an angle 2θ.[8] The three partial structure functions for water (a_{OO}, a_{OH}, a_{HH}) may be obtained from neutron diffraction experiments on at least three different isotopic mixtures. Such experiments were recently reported by Thiessen and Narten whose work has high statistical accuracy achieved by counting very large numbers of neutrons.[8] Even so, the analyses of the data are hampered by the need to remove large contributions from inelastic and incoherent scattering. The determination of the radial distribution functions by inverting Eq. (3) is further impeded by substantial termination effects.

With this in mind, the Monte Carlo and experimental results are compared in Figs. 1–12. In each case the dashed curves are the experimental data; the partial structure functions are taken from Figs. 8–10 in Thiessen's and Narten's paper[8] and only include intermolecular scattering, while the experimental g_{OO} is from the x-ray experiments of Narten and Levy.[21] It should be noted that the OO partial structure functions from the neutron and x-ray experiments are in excellent accord.[8,21] Another point to note is that the experimental data for the partial structure functions are not reliable in the small angle region below about $k = 1$ Å^{-1}. The theoretical results below 1 Å^{-1} are also highly dependent on the cutoff distance, though no significant difference is found in the results above 1 Å^{-1} from the simulations for $N = 125$ or 216 with the TIP4P potential. Experimental OH and HH radial distribution functions have not been shown due to the uncertainties in inverting Eq. (3) as mentioned above. The problem is illustrated by the g_{OH}

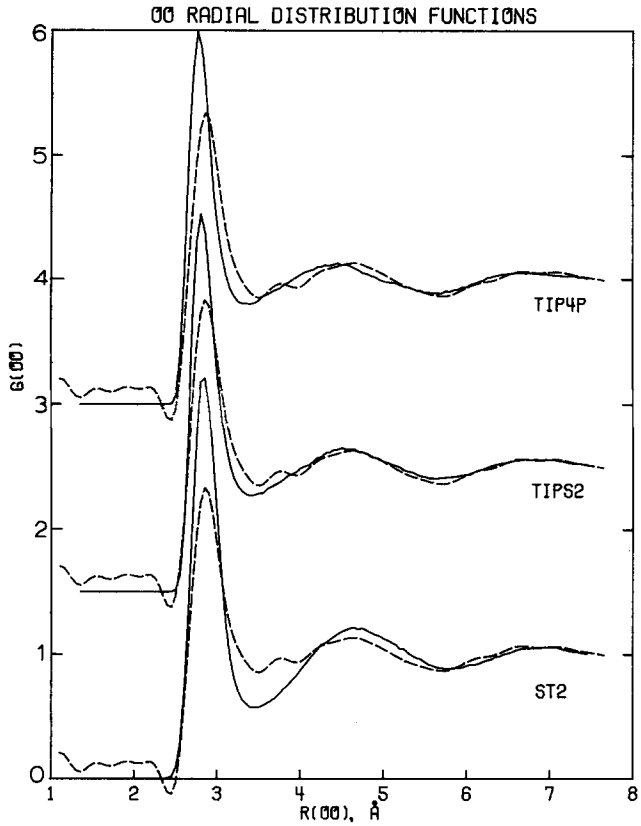

FIG. 1. Oxygen–oxygen radial distribution functions. The dashed line shows the x-ray results (Ref. 21).

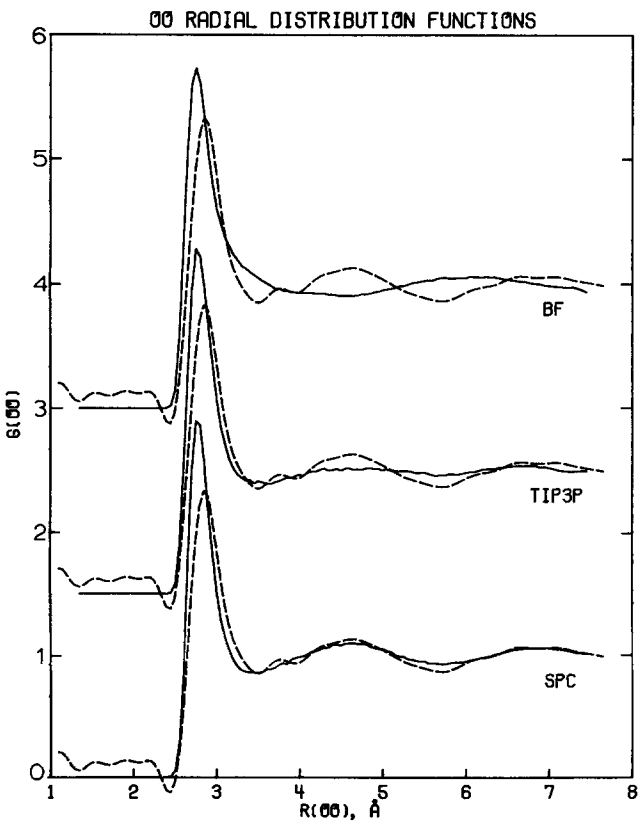

FIG. 2. Oxygen–oxygen radial distribution functions. The dashed line shows the x-ray results (Ref. 21).

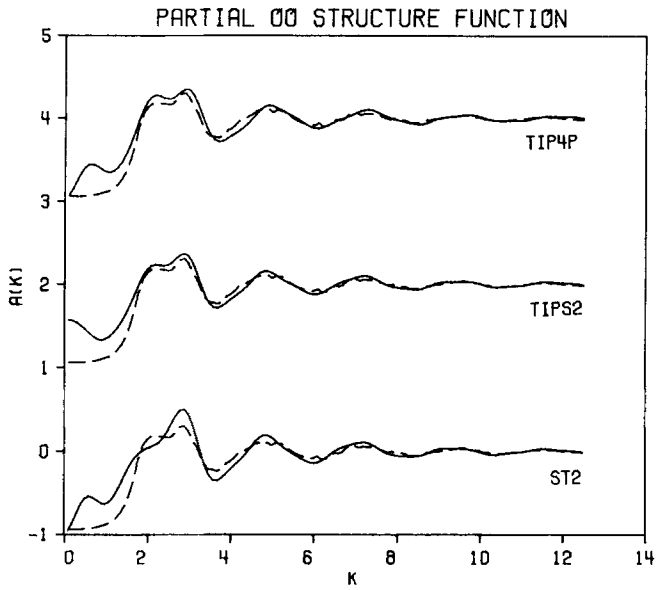

FIG. 3. Oxygen–oxygen partial structure functions. Experimental neutron data (dashed lines) are from Ref. 8. Units for k are $Å^{-1}$ throughout.

and g_{HH} recently reported by Narten, Thiessen, and Blum from the neutron data.[22] The results are much more structured than Narten's earlier neutron findings,[23] other experimental results[24] and the outcomes of all reasonable theoretical studies.

The computed OO radial distribution functions (Figs. 1 and 2) all have first peaks significantly higher than the x-ray result with the ST2 potential having the highest peak height (3.2). The first peak may be integrated to obtain the number of nearest neighbors for a monomer. With an integration limit of 3.5 Å, the experimental value is 5.0 and the potential functions yield 5.1 (SPC), 5.2 (TIP3P), 6.9 (BF), 4.8 (TIPS2), 5.1 (TIP4P), and

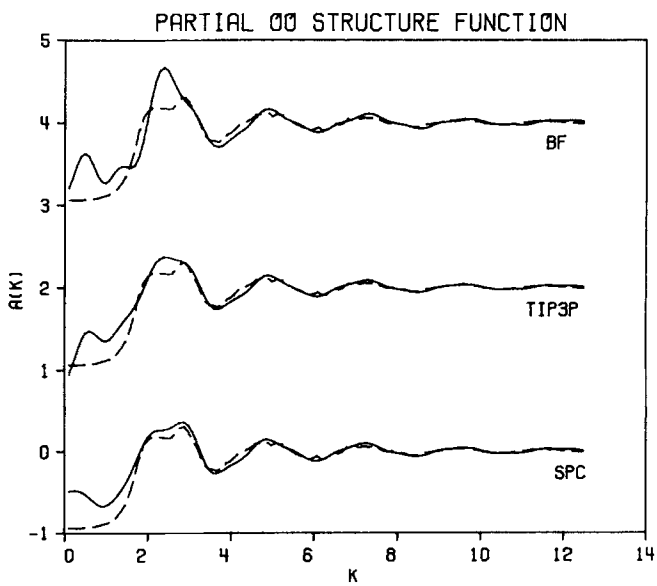

FIG. 4. Oxygen–oxygen partial structure functions as in Fig. 3.

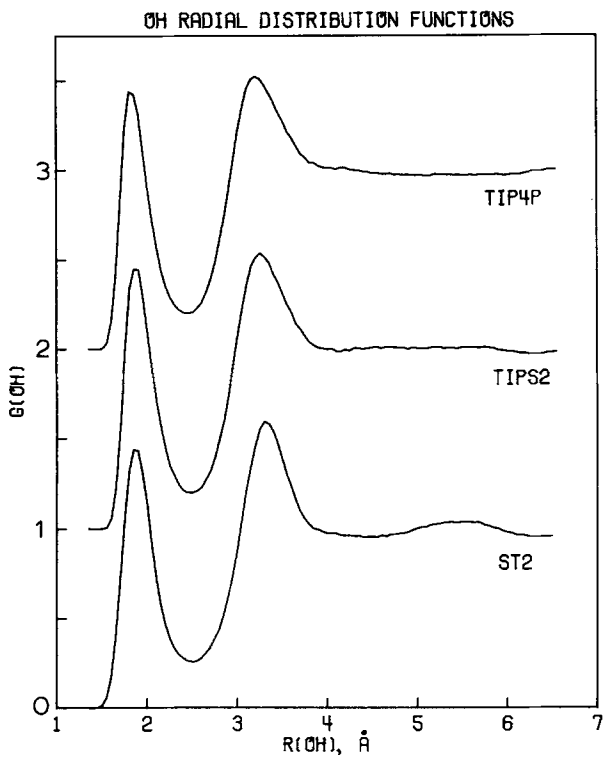

FIG. 5. Oxygen–hydrogen radial distribution functions.

4.9 (ST2). The only serious error is for the BF potential which is consistent with its overestimate of the density. Overall, the closest agreement with experiment for g_{OO} is given by the TIPS2 and SPC potentials.

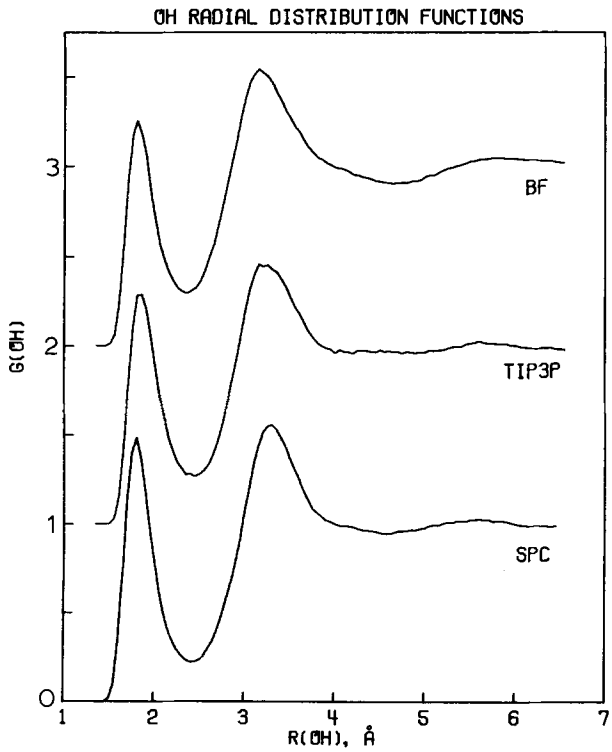

FIG. 6. Oxygen–hydrogen radial distribution functions.

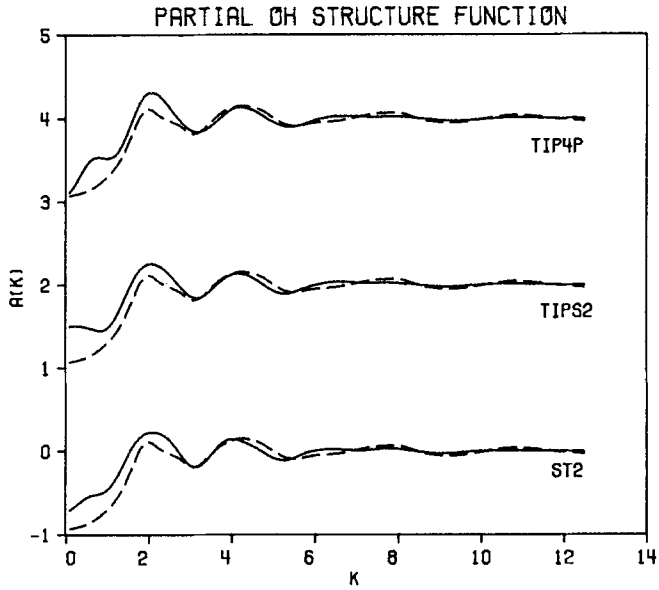

FIG. 7. Oxygen–hydrogen partial structure functions as in Fig. 3.

The TIP4P results are also quite good, though the peak positions are shifted in a little. The ST2 prediction is overly structured which has been noted previously,[2,5] while TIP3P gives too little structure beyond the first peak. This appears to be a general problem for the 3-site models; as the density is improved from the SPC value, the second peak is progressively flattened. Increasing the density has a similar effect on the 4-site models, however, it is less severe and their results are more structured to begin with. Thus, the TIP4P potential which has the correct density still gives good second and third peaks in g_{OO}. The g_{OO} from the BF potential is poor with the second peak severely mis-

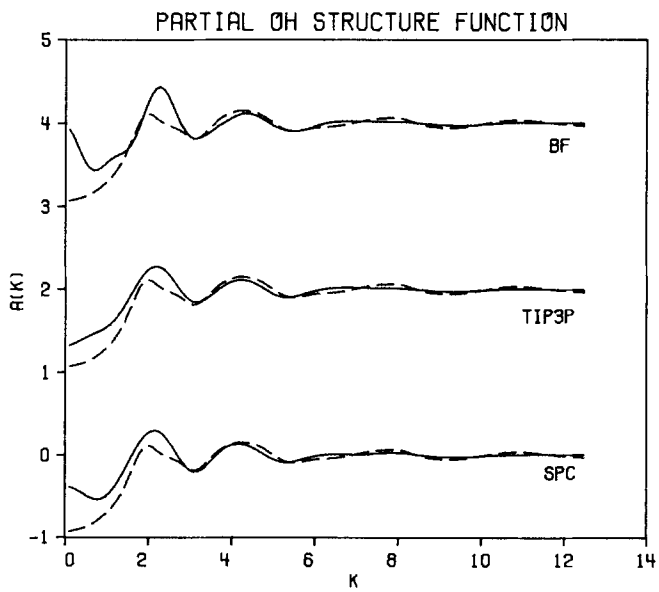

FIG. 8. Oxygen–hydrogen partial structure functions as in Fig. 3.

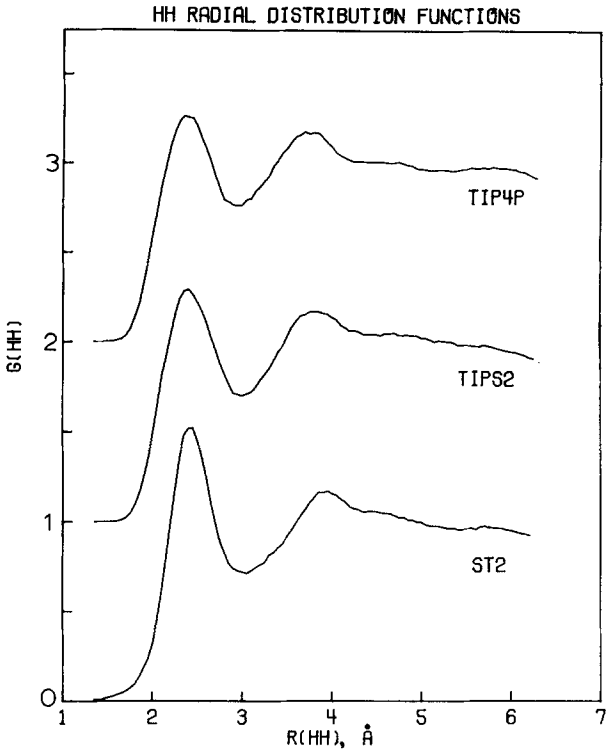

FIG. 9. Hydrogen–hydrogen radial distribution functions.

placed. Though this model is important from a historical standpoint, there is now no justification for using the original parametrization in fluid simulations. In *NPT* simulations it yields unacceptable densities and structure, and in *NVT* simulations excessively negative pressures are obtained.

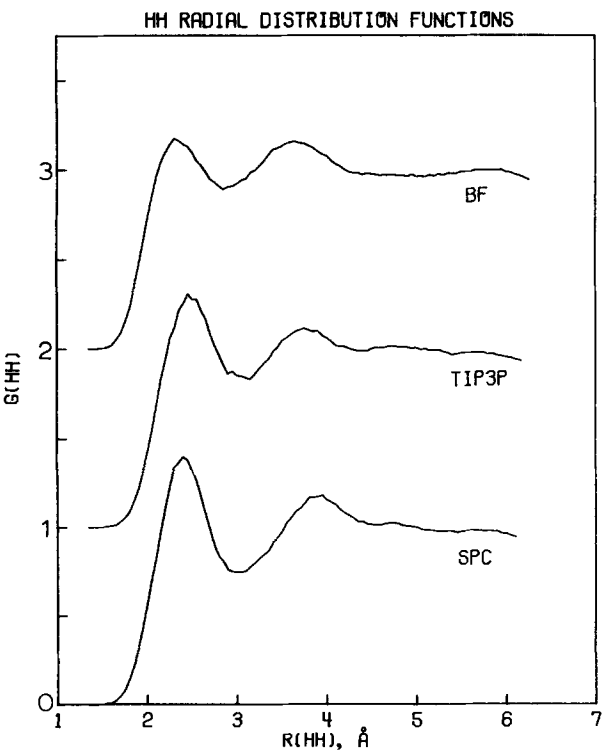

FIG. 10. Hydrogen–hydrogen radial distribution functions.

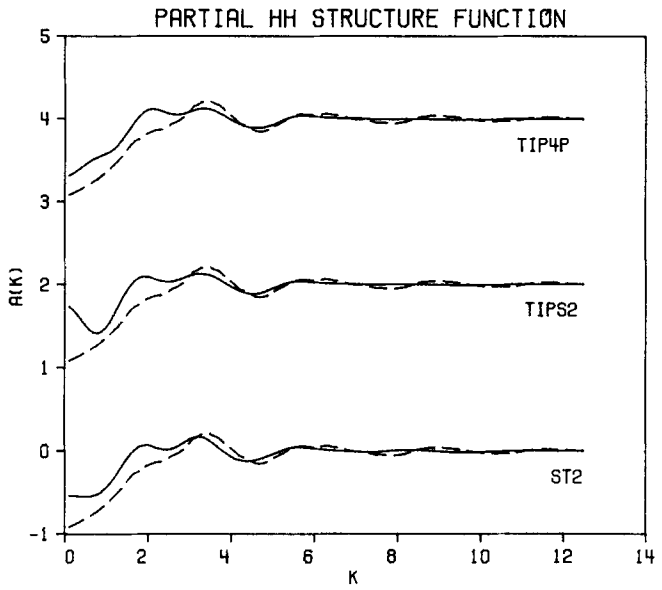

FIG. 11. Hydrogen–hydrogen partial structure functions as in Fig. 3.

The OO partial structure functions are displayed in Figs. 3 and 4. The TIPS2, TIP4P, and SPC potentials are again found to yield the best results. In particular, the TIPS2 and TIP4P functions nicely mirror the double peak in the neutron results at 2.5 $Å^{-1}$. This is the most discerning feature in a_{OO}, though the connection between its shape and the form of g_{OO} is not clearly evident. However, the double peak appears to merge as the second peak near 4.5 Å in g_{OO} is diminished as in going from SPC to TIP3P to BF. In addition, the greater structure in g_{OO} for the ST2 potential is carried over into a_{OO}. The close agreement between the TIPS2,

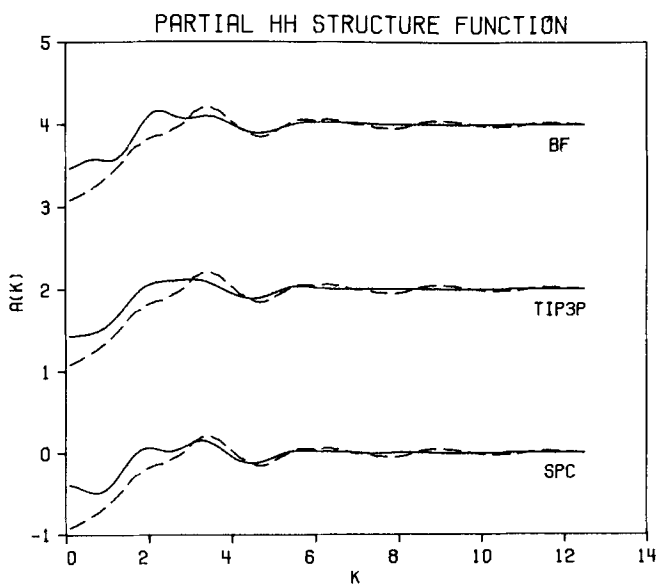

FIG. 12. Hydrogen–hydrogen partial structure functions as in Fig. 3.

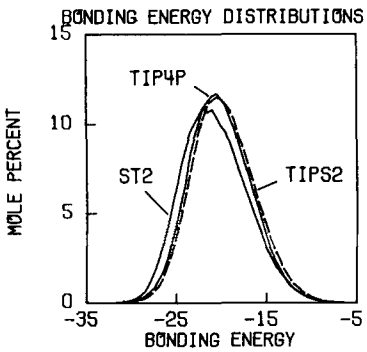

FIG. 13. Distributions of total bonding energies for monomers in liquid water. Energy in kcal/mol. Units for the ordinate are mol% per kcal/mol.

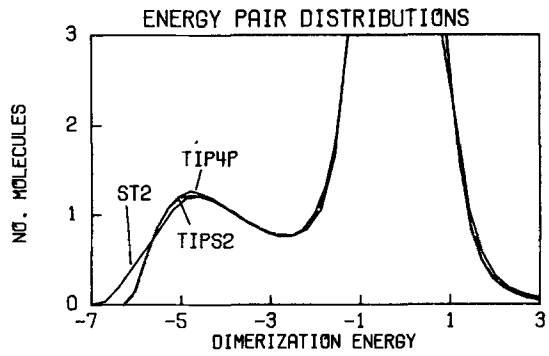

FIG. 15. Distributions of dimerization energies (kcal/mol) for monomers in liquid water. Units for the ordinate are number of molecules per kcal/mol.

TIP4P, and experimental findings for a_{OO}, yet the differences in the g_{OO}'s, particularly for the first peak, illustrate the sensitivity of the inversion of Eq. (3).

The most striking feature about the OH and HH radial distribution functions in Figs. 5, 6, 9, and 10 is the similarity of the computed results. In each case for g_{OH} two strong peaks are obtained at about 1.9 and 3.3 Å with the second a little higher. Integration of the first peak to 2.5 Å yields the following estimates for the average number of hydrogen bonds per monomer: 3.9 (SPC), 3.9 (TIP3P), 4.5 (BF), 3.8 (TIPS2), 3.9 (TIP4P), and 4.1 (ST2). A little more variety is found for the computed HH radial distribution functions, though again two well defined peaks near 2.4 and 3.8 Å are apparent in each case. These features are also found in the experimental results for g_{OH} and g_{HH}; however, the precise location and heights for the peaks are uncertain.[22-24]

Not surprisingly, the computed OH partial structure functions in Figs. 7 and 8 are also similar. The agreement with the neutron data is not as good as for a_{OO}. In particular, the height of the peak near 2 Å^{-1} is consistently overestimated and the oscillations at large k are less pronounced than the experimental results and a little out of phase. The accord appears to worsen for the HH partial structure function (Figs. 11 and 12). The potential functions except TIP3P yield double peaks at 2 and 3.5 Å^{-1}, while the former is a lower shoulder in the experimental curve. It may not be justified to assign too much significance to the discrepancies near 2 Å^{-1} since this is on the edge of the low angle region where the accuracy of the neutron results is diminished.

In summary, the results for the OO distributions are quite good for the TIPS2, TIP4P, and SPC potential functions. The results for the OH and HH distributions appear to be less acceptable, though they suggest that the TIP4P potential which gives excellent thermodynamic results, the correct density and proper placement of the oxygens, simultaneously has the hydrogens somewhat misplaced. This is conceivable particularly in view of the neglect of specific three-body interactions with the potential functions. However, considering the history of the diffraction results and the uncertainties in making the incoherent and inelastic scattering and other corrections,[8,21-24] attempts to modify the potential functions to yield closer accord with the neutron partial structure functions are not clearly warranted at this time.

D. Energy and hydrogen bonding distributions

The distributions of total intermolecular bonding energies obtain from the Monte Carlo calculations are presented in Figs. 13 and 14. In each case the monomers are found to experience a continuum of energetic environments covering a range of about 20 kcal/mol.

The shapes of the energy pair distributions (Figs. 15 and 16), which represent the distribution of dimer-

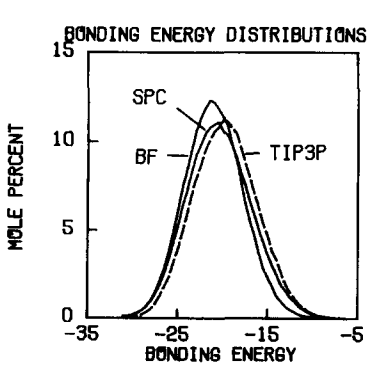

FIG. 14. Total bonding energy distributions as in Fig. 13.

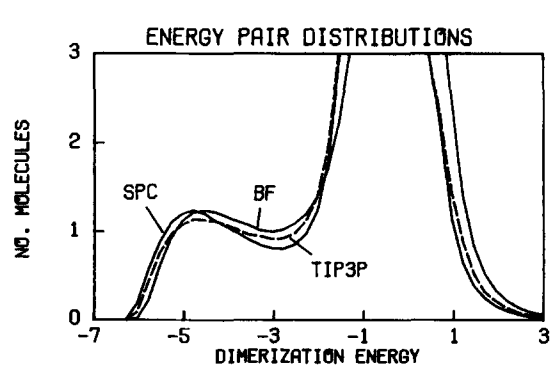

FIG. 16. Distributions of dimerization energies as in Fig. 15.

TABLE IV. Results of hydrogen bond analyses for liquid water at 25°C and 1 atm.[a]

	SPC	TIP3P	BF	TIPS2	TIP4P	ST2
No. of H bonds	3.54	3.50	3.73	3.54	3.57	3.67
ϵ (H bond)	−4.34	−4.20	−3.95	−4.15	−4.17	−4.26
ϵ (Coulomb)	−5.65	−5.39	−4.82	−5.52	−5.52	−4.59
ϵ (LJ)	1.31	1.19	0.87	1.37	1.35	0.34
θ, deg	156	155	154	158	158	153
ϕ, deg	99	100	96	99	99	101
% monomers in N H bonds						
$N=0$	0.0	0.0	0.0	0.0	0.0	0.0
$N=1$	1.0	1.3	0.9	0.9	0.8	0.7
$N=2$	9.6	10.9	7.9	9.5	8.8	6.8
$N=3$	34.1	35.7	29.5	33.0	33.7	29.4
$N=4$	46.2	41.5	43.2	47.8	46.8	52.1
$N=5$	8.6	9.9	16.4	8.3	9.5	10.4
$N=6$	0.6	0.7	2.0	0.4	0.4	0.7

[a] ϵ's in kcal/mol. ϵ (H bond) is the average hydrogen bond energy which can be decomposed into Coulomb ϵ (Coulomb) and Lennard-Jones ϵ(LJ) terms. A hydrogen bond is defined by an interaction energy of −2.25 kcal/mol or less.

ization energies experienced by a monomer, are also similar. The low energy band represents the hydrogen bonded neighbors, while the spike near 0 kcal/mol includes the many distant molecules in the bulk. The minimum near −2.5 kcal/mol is not as deep for the 3-site and BF potentials. This implies that the hydrogen bonded neighbors are distinguished less from second neighbors with these models. The similarity of the TIPS2, TIP4P, and ST2 results (Fig. 15) is also notable; the only difference is at the lowest energies which reflects the greater maximal hydrogen bond strength for the ST2 potential (Table II).

As used in the past, the location of the minimum in the energy pair distributions suggests a convenient energetic definition of a hydrogen bond. For the present purposes any pair of molecules bound by at least 2.25 kcal/mol is considered to be hydrogen bonded. Analyses of the hydrogen bonding were then made from configurations saved at regular intervals during the Monte Carlo runs. The key results are summarized in Table IV. With this definition, the average number of hydrogen bonds ranges from 3.50 to 3.73 which is a little less than from integrating the first peak in the OH radial distribution functions. The average hydrogen bond strengths are −3.95 to −4.34 kcal/mol and can be decomposed into Lennard-Jones and Coulombic contributions in view of the form of Eq. (1). The components are generally similar, though the hydrogen bonds for the ST2 potential involve both less electrostatic attraction and less short range repulsion than for the other potential functions.

The angles θ and ϕ refer to the O–H$\cdots$O hydrogen bond angle and the H$\cdots$O–H angle between the hydrogen bond donor and acceptor, respectively. Only the average values are given in Table IV, though the full distributions for θ and ϕ have been reported previously.[4,25] Both the averages and full distributions are nearly the same for all six potential functions. The hydrogen bonds are bent an average of 20°–25° from linear.

The percentage of monomers in N hydrogen bonds is also recorded for each potential function in Table IV. The results are generally similar, though the ST2 potential shows the strongest preference for monomers to participate in four hydrogen bonds. This is consistent with the tetrahedral charge distribution used in the ST2 potential and the greater structure found for its radial distribution functions. All potential functions except BF place 77%–81% of the monomers in three or four hydrogen bonds. The BF potential yields 73%, but it has a higher percentage of monomers with more than four hydrogen bonds. Coupled with its weaker average hydrogen bond strength, it is clear that the higher density of BF water is accompanied by less icelike, tetrahedral structure than for the other models and real water. Overall, except for the BF model, the computed energetic descriptions and hydrogen bonding characteristics are consistent and remarkably similar quantitatively.

V. CONCLUSION

The results of Monte Carlo simulations for liquid water at 25 °C and 1 atm using six simple potential functions have been compared with experimental thermodynamic and structural data. The only potential function that was clearly found to be poor is the original BF model. The other five potential functions all provide reasonable descriptions of liquid water and should be useful in simulations of aqueous solutions. A case can be made

that the TIPS2 and TIP4P potentials are the most promising overall. They both yield an excellent a_{OO} in comparison to diffraction data as well as good thermodynamic results. Furthermore, their simple form allows rapid evaluation. The TIPS2 potential appears to yield slightly better peak positions for g_{OO}, while TIP4P gives an uncorrected density in exact agreement with experiment for water at 25 °C and 1 atm. The latter feature is attractive for *NPT* simulations of aqueous solutions. The ST2 potential is slower to evaluate and yields too much structure in the OO distributions. However, in molecular dynamics simulations the ST2 potential yields a somewhat better self-diffusion constant than the 3- or 4-site models. In general the 3-site potentials provide too little structure in g_{OO} beyond the first peak and the problem intensifies as the density is improved.

Comparisons have only been made here for liquid water at 25 °C and 1 atm. It would be remarkable for models as simple as those considered here to be equally successful without reparametrization for different phases under widely varying conditions.[1] In view of the interest in and importance of aqueous solutions near 25 °C and 1 atm, several of the potential functions discussed here clearly provide a useful and valuable basis for computer simulation of many fascinating systems.

ACKNOWLEDGMENTS

Gratitude is expressed to the National Science Foundation (Grant CHE-8020466) for support of this work. The authors are also grateful To Dr. M. Mezei, Dr. A. H. Narten, and Dr. K. R. Wilson for helpful discussions and preprints.

[1]J. R. Reimers, R. O. Watts, and M. L. Klein, Chem. Phys. **64**, 95 (1982).
[2]D. L. Beveridge, M. Mezei, P. K. Mehrotra, F. T. Marchese, G. Ravi-Shanker, T. Vasu, and S. Swaminathan, in *Advances in Chemistry* (American Chemical Society, Washington, D.C., 1983).
[3]W. L. Jorgensen, J. Am. Chem. Soc. **103**, 335 (1981).
[4]W. L. Jorgensen, J. Chem. Phys. **77**, 4156 (1982).
[5]F. H. Stillinger and A. Rahman, J. Chem. Phys. **60**, 1545 (1974).
[6]J. D. Bernal and R. H. Fowler, J. Chem. Phys. **1**, 515 (1933).
[7]H. J. C. Berendsen, J. P. M. Postma, W. F. von Gunsteren, and J. Hermans, in *Intermolecular Forces*, edited by B. Pullman (Reidel, Dordrecht, Holland, 1981), p. 331.
[8]W. E. Thiessen and A. H. Narten, J. Chem. Phys. **77**, 2656 (1982).
[9]T. R. Dyke and J. S. Muenter, J. Chem. Phys. **60**, 2929 (1974); J. A. Odutola and T. R. Dyke, *ibid.* **72**, 5062 (1980).
[10]L. A. Curtiss, D. J. Frurip, and M. Blander, J. Chem. Phys. **71**, 2703 (1979).
[11]I. R. McDonald, Mol. Phys. **23**, 41 (1972).
[12](a) G. S. Kell, J. Chem. Eng. Data **20**, 97 (1975); (b) N. E. Dorsey, *Properties of Ordinary Water Substances* (Rheinhold, New York, 1940); (c) R. Mills, J. Phys. Chem. **77**, 685 (1973).
[13]W. L. Jorgensen, Chem. Phys. Lett. **92**, 405 (1982).
[14]J. C. Owicki and H. A. Scheraga, J. Am. Chem. Soc. **99**, 7403 (1977).
[15]M. Mezei and D. L. Beveridge, J. Chem. Phys. **76**, 593 (1982).
[16]F. H. Stillinger and A. Rahman, J. Chem. Phys. **68**, 666 (1978).
[17]M. Mezei, S. Swaminathan, and D. L. Beveridge, J. Chem. Phys. **71**, 3366 (1979).
[18]C. Pangali, M. Rao, and B. J. Berne, Mol. Phys. **40**, 661 (1980).
[19]G. C. Lie, E. Clementi, and M. Yoshimine, J. Chem. Phys. **64**, 2314 (1976).
[20]P. H. Berens, D. H. J. Mackay, G. M. White, and K. R. Wilson, J. Chem. Phys. (in press).
[21]A. H. Narten and H. A. Levy, J. Chem. Phys. **55**, 2263 (1971).
[22]A. H. Narten, W. E. Thiessen, and L. Blum, Science **217**, 1033 (1982).
[23]A. H. Narten, J. Chem. Phys. **56**, 5681 (1972).
[24]G. Palinkas, E. Kalman, and P. Kovacs, Mol. Phys. **34**, 525 (1977); A. K. Soper and R. N. Silver, Phys. Rev. Lett. **49**, 471 (1982).
[25]W. L. Jorgensen, Chem. Phys. Lett. **70**, 326 (1980).